



# LUND UNIVERSITY

## Asymptotic Analysis of Spatially Coupled MacKay-Neal and Hsu-Anastasopoulos LDPC Codes

Mitchell, David G.M.; Kasai, Kenta; Lentmaier, Michael; Costello Jr., Daniel J.

*Published in:*  
2012 International Symposium on Information Theory and its Applications

2012

[Link to publication](#)

### *Citation for published version (APA):*

Mitchell, D. G. M., Kasai, K., Lentmaier, M., & Costello Jr., D. J. (2012). Asymptotic Analysis of Spatially Coupled MacKay-Neal and Hsu-Anastasopoulos LDPC Codes. In *2012 International Symposium on Information Theory and its Applications* (pp. 337-341). IEEE - Institute of Electrical and Electronics Engineers Inc..  
<http://ieeexplore.ieee.org/stamp/stamp.jsp?tp=&arnumber=6400949>

*Total number of authors:*  
4

### General rights

Unless other specific re-use rights are stated the following general rights apply:  
Copyright and moral rights for the publications made accessible in the public portal are retained by the authors and/or other copyright owners and it is a condition of accessing publications that users recognise and abide by the legal requirements associated with these rights.

- Users may download and print one copy of any publication from the public portal for the purpose of private study or research.
- You may not further distribute the material or use it for any profit-making activity or commercial gain
- You may freely distribute the URL identifying the publication in the public portal

Read more about Creative commons licenses: <https://creativecommons.org/licenses/>

### Take down policy

If you believe that this document breaches copyright please contact us providing details, and we will remove access to the work immediately and investigate your claim.

LUND UNIVERSITY

PO Box 117  
221 00 Lund  
+46 46-222 00 00

# Asymptotic Analysis of Spatially Coupled MacKay-Neal and Hsu-Anastasopoulos LDPC Codes

David G. M. Mitchell\*, Kenta Kasai†, Michael Lentmaier‡, and Daniel J. Costello, Jr.\*

†Dept. of Electrical Engineering, University of Notre Dame, Notre Dame, Indiana, USA,  
{david.mitchell, costello.2}@nd.edu

†Dept. of Communications and Integrated Systems, Tokyo Institute of Technology 152-8550 Tokyo, Japan  
kenta@comm.ss.titech.ac.jp

‡Vodafone Chair Mobile Communications Systems, Dresden University of Technology, Dresden, Germany,  
michael.lentmaier@ifn.et.tu-dresden.de

**Abstract**—MacKay-Neal (MN) and Hsu-Anastasopoulos (HA) low-density parity-check (LDPC) codes are known to achieve the capacity of memoryless binary-input symmetric-output channels under maximum likelihood (ML) decoding with bounded column and row weight in their associated parity-check matrices. Recently, Kasai and Sakaniwa showed that spatially coupled (SC) versions of the MN and HA LDPC codes have belief propagation (BP) iterative decoding thresholds that approach capacity on the binary erasure channel (BEC) as the coupling length increases.

In this paper, we extend the results of Kasai and Sakaniwa to the additive white Gaussian noise (AWGN) channel and show that the thresholds of the SC-MN and SC-HA ensembles approach capacity with bounded density as the coupling length increases, i.e., the number of edges per information bit approaches a finite value as the estimated BP threshold approaches the Shannon limit. We also perform an asymptotic weight enumerator analysis and show that, provided the density parameters are chosen to be sufficiently large, the SC-MN and SC-HA ensembles are asymptotically good. Further, for certain selections of parameters, some of these ensembles are shown to have both excellent thresholds and good distance properties.

## I. INTRODUCTION

Ensembles of spatially coupled low-density parity-check codes (SC-LDPCCs) can be obtained by terminating LDPC convolutional code ensembles [1]. The reduced check node degrees resulting from the termination of the convolutional codes have been shown to lead to substantially better belief propagation (BP) decoding thresholds compared to corresponding block, or *uncoupled*, code ensembles [1]–[6]. It has been proven analytically for the binary erasure channel (BEC) that the BP decoding thresholds of a class of  $(J, K)$ -regular SC-LDPCC ensembles achieve the maximum a posteriori probability (MAP) decoding thresholds of the corresponding  $(J, K)$ -regular LDPC block code ensembles [5]. This phenomenon has been termed “threshold saturation” and has recently been proven for general memoryless binary-input symmetric-output (MBS) channels [6].

As a result of threshold saturation, the  $(J, K)$ -regular SC-LDPCC ensembles studied in [5] and [6] achieve capacity *universally* on MBS channels with BP decoding as the variable and check node degrees  $J$  and  $K$  increase, since, for an arbitrary MBS channel, the MAP thresholds of the corresponding block code ensembles improve to the Shannon limit [7].

However, the *density* of a rate  $R = 1 - J/K$ ,  $(J, K)$ -regular LDPC code ensemble, defined as the number of edges per information bit, is given by  $JK/(K - J)$ , which is unbounded as  $J, K \rightarrow \infty$ .

In comparison to many other capacity approaching constructions, MacKay-Neal (MN) [8], [9] and Hsu-Anastasopoulos (HA) [10] LDPC codes can be shown to achieve capacity on MBS channels with *bounded* density under maximum likelihood (ML) decoding [10]–[12]. This is achieved by puncturing a number of the variable nodes in the Tanner graph of the code. MN codes are non-systematic LDPC codes, with two different edge types. HA codes, the duals of MN codes, are constructed by concatenating LDPC codes and low-density generator-matrix (LDGM) codes. In [13], Kasai and Sakaniwa showed that spatially coupled versions of the MN and HA LDPC codes have BP thresholds that approach capacity on the BEC as the coupling length increases.

In this paper, we extend the results of [13] to the additive white Gaussian noise (AWGN) channel and show that the BP thresholds of the SC-MN and SC-HA ensembles approach capacity with bounded density as the coupling length increases, i.e., the number of edges per information bit approaches a finite value as the estimated BP threshold approaches the Shannon limit. We also perform an asymptotic weight enumerator analysis and show that, provided the density parameters are chosen to be sufficiently large, the SC-MN and SC-HA ensembles are *asymptotically good*, i.e., the minimum distance typical of most members of the ensemble grows linearly with block length as the block length tends to infinity. Further, for certain selections of parameters, some of these ensembles are shown to have both excellent thresholds and large minimum distance growth rates.

## II. PROTOGRAPH-BASED SPATIALLY COUPLED LDPC CODE ENSEMBLES

### A. Protograph construction of LDPC codes

A protograph [14] is a small bipartite graph  $B = (V, C, E)$  that connects a set of  $n_v$  variable nodes to a set of  $n_c$  check nodes by a set of edges  $E$ . The protograph can be represented by a parity-check or *base* biadjacency matrix  $\mathbf{B}$ , where  $B_{x,y}$  is taken to be the number of edges connecting variable node  $v_y$  to check node  $c_x$ . The parity-check matrix  $\mathbf{H}$  of a protograph-based LDPC block code can be created by replacing each

non-zero entry in  $\mathbf{B}$  by a sum of  $B_{x,y}$  permutation matrices of size  $N$  and a zero entry by the  $N \times N$  all-zero matrix. It is an important feature of this construction that each derived code inherits the degree distribution and graph neighbourhood structure of the protograph. The ensemble of protograph-based LDPC codes with block length  $n = Nn_v$  is defined by the set of matrices  $\mathbf{H}$  that can be derived from a given protograph by all possible combinations of  $N \times N$  permutation matrices.

### B. Spatially coupled protographs

SC-LDPC code ensembles can be constructed by *coupling* together several block code ensembles in a chain. Figure 1 shows representative Tanner graphs for (a) an LDPC block code ensemble, (b) an uncoupled chain of LDPC block code ensembles, and (c) a SC-LDPC code ensemble.

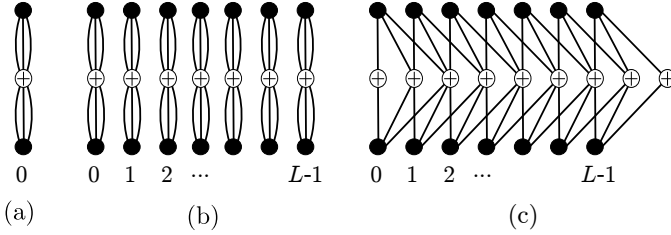


Fig. 1. Tanner graphs associated with (a) a (3,6)-regular LDPC block code protograph, (b) a chain of  $L$  uncoupled (3,6)-regular LDPC block code protographs for  $L = 7$ , and (c) a chain of  $L$  spatially coupled (3,6)-regular LDPC block code protographs for  $L = 7$ .

For the (3,6)-regular ensemble depicted in Fig. 1(a), the iterative decoding threshold for the BEC is  $\epsilon_{BP} = 0.4294$ . Figure 1(b) shows a chain of  $L$  uncoupled (3,6)-regular LDPC block code protographs. This figure corresponds to block code transmission over time. Here, at each time unit  $t = 0, 1, \dots, L-1$ , a block of data of length  $2N$  is transmitted and decoded independently. As a result of the noninteracting structure, each component behaves like the original protograph in Fig. 1(a) and the BP threshold of each protograph is  $\epsilon_{BP} = 0.4294$ .

By coupling together the block code protographs, as demonstrated in Fig. 1(c) for  $L = 7$ , we obtain the protograph of a SC-LDPCC ensemble. Note that, by coupling the protographs in this way, we introduce a “structured irregularity” into the coupled protograph; in this example all of the variable nodes still have 3 edge connections, however the check nodes at the start and the end of the chain have fewer than 6 connections. For this example of a (3,6)-regular SC-LDPC code ensemble, the threshold saturation effect improves the BP threshold from the uncoupled BP threshold  $\epsilon_{BP} = 0.4294$  to the (optimal) MAP threshold  $\epsilon_{MAP} = 0.4881$  as the coupling length  $L$  becomes sufficiently large.

The base matrix of a SC-LDPCC ensemble is given by

$$\mathbf{B}_{[0,L-1]} = \begin{bmatrix} \mathbf{B}_0 & & & \\ \vdots & \ddots & & \\ \mathbf{B}_{m_s} & & \mathbf{B}_0 & \\ & & \ddots & \vdots \\ & & & \mathbf{B}_{m_s} \end{bmatrix}_{(L+m_s)b_c \times Lb_v}. \quad (1)$$

where  $m_s + 1$  is the *coupling width*,<sup>1</sup> and the  $b_c \times b_v$  *component base matrices*  $\mathbf{B}_i$ ,  $i = 0, \dots, m_s$ , represent the edge connections from the  $b_v$  variable nodes in segment  $t$  to the  $b_c$  check nodes in segment  $t+i$ . Starting from the base matrix  $\mathbf{B}$  of a block code ensemble with design rate  $R = 1 - b_c/b_v$ , one can construct the base matrix of a SC-LDPCC ensemble that has (asymptotically, for large  $L$ ) the same degree distribution and structure as the original ensemble. This is achieved by an *edge spreading* procedure (see [1] for details) that divides the edges from each variable node in the base matrix  $\mathbf{B}$  among  $m_s + 1$  component base matrices  $\mathbf{B}_i$ ,  $i = 0, \dots, m_s$ , such that the condition  $\mathbf{B}_0 + \mathbf{B}_1 + \dots + \mathbf{B}_{m_s} = \mathbf{B}$  is satisfied. For example, the (3,6)-regular example given above can be constructed by spreading the edges of  $\mathbf{B} = \begin{bmatrix} 3 & 3 \end{bmatrix}$  as  $\mathbf{B}_0 = \begin{bmatrix} 1 & 1 \end{bmatrix} = \mathbf{B}_1 = \mathbf{B}_2$ , where  $m_s = 2$ .

As a result of the boundary effects of spatial coupling, we observe some rate loss. Without puncturing, the design rate  $R_L$  of the SC-LDPCC ensemble is equal to

$$R_L = 1 - \left( \frac{L + m_s}{L} \right) (1 - R).$$

Note that, as the coupling length  $L$  increases, the rate increases and approaches the rate  $R = 1 - b_c/b_v$  of the block code ensemble as  $L \rightarrow \infty$ .

## III. SPATIALLY COUPLED MACKAY-NEAL AND HSU-ANASTASOPOULOS LDPC CODE ENSEMBLES

We follow the construction of SC-MN and SC-HA protographs presented in [13]. The constructions are designed such that the SC-MN and SC-HA constructions have the same column-weight and almost the same row-weight distributions as the corresponding MN and HA construction, respectively. The protographs of SC-MN and SC-HA ensembles will be constructed from several simple terminated LDPC convolutional code base matrices.

### A. SC-MN LDPCC ensembles

Let  $J = kK$ ,  $J, K \geq 2$ ,  $g \in [2, 2k + J]$ , and  $L \geq 1$ , for  $J, K, g, L, k \in \mathbb{Z}$ . We construct the base matrix of a  $(J, K, g, L)$  SC-MN LDPCC ensemble by concatenating two SC-LDPCC base matrices  $\mathbf{V}_{[0,2L]}$  and  $\mathbf{S}_{[0,k(2L+K)-g]}$ , in the form of (1), where the component submatrices  $\mathbf{V}_i$ ,  $i = 0, \dots, K-1$ , are each the all-ones matrix of size  $k \times 1$  and the submatrices  $\mathbf{S}_j$ ,  $j = 0, \dots, g-1$ , are each the all-ones matrix of size  $1 \times 1$ , respectively. Consequently,  $\mathbf{V}_{[0,2L]}$  has size  $k(2L + K) \times (2L + 1)$  and  $\mathbf{S}_{[0,k(2L+K)-g]}$  has size  $k(2L + K) \times (k(2L + K) - g + 1)$ . Then the base matrix of a  $(J, K, g, L)$  SC-MN LDPCC ensemble can be written as

$$\mathbf{B}_{[0,L-1]}^{MN} = \begin{bmatrix} \mathbf{V}_{[0,2L]} & \mathbf{S}_{[0,k(2L+K)-g]} \end{bmatrix}, \quad (2)$$

where the variable nodes associated with  $\mathbf{V}_{[0,2L]}$  are punctured. The design rate of the ensemble is given by

$$R^{MN}(J, K, g, L) = \frac{2L - g + 2}{k(2L + 1) + J - g - 1}, \quad (3)$$

<sup>1</sup>The value  $m_s$  denotes the *syndrome former memory* of the associated (unterminated) convolutional code ensemble.

where

$$\lim_{L \rightarrow \infty} R^{MN}(J, K, g, L) = \frac{1}{k},$$

and the number of edges per information bit, or *density*, of members of the ensemble is given by

$$\rho^{MN}(J, K, g, L) = \frac{J(2L+1) + g(2kL + J - g + 1)}{2(L+1) - g}, \quad (4)$$

with

$$\lim_{L \rightarrow \infty} \rho^{MN}(J, K, g, L) = J + gk.$$

For example, consider the  $(4, 2, 2, 2)$  SC-MN LDPCC ensemble. Here,  $k = J/K = 2$ ,  $R^{MN}(4, 2, 2, 2) = 4/11$ , and  $\rho^{MN}(4, 2, 2, 2) = 21/2$ . The component submatrices are given as

$$\mathbf{V}_0 = \mathbf{V}_1 = \begin{bmatrix} 1 \\ 1 \end{bmatrix} \text{ and } \mathbf{S}_0 = \mathbf{S}_1 = \begin{bmatrix} 1 \end{bmatrix},$$

which are used to construct the base matrix of the  $(4, 2, 2, 2)$  SC-MN ensemble as follows:

$$\mathbf{B}_{[0, L-1]}^{MN} = \mathbf{B}_{[0, 1]}^{MN} = \left[ \mathbf{V}_{[0, 4]} \mid \mathbf{S}_{[0, 10]} \right] = \begin{bmatrix} 1 & 0 & 0 & 0 & 0 & 1 & 0 & 0 & 0 & 0 & 0 & 0 & 0 & 0 & 0 & 0 & 0 & 0 & 0 & 0 \\ 1 & 0 & 0 & 0 & 0 & 1 & 1 & 0 & 0 & 0 & 0 & 0 & 0 & 0 & 0 & 0 & 0 & 0 & 0 & 0 \\ 1 & 1 & 0 & 0 & 0 & 0 & 1 & 1 & 0 & 0 & 0 & 0 & 0 & 0 & 0 & 0 & 0 & 0 & 0 & 0 \\ 1 & 1 & 0 & 0 & 0 & 0 & 0 & 1 & 1 & 0 & 0 & 0 & 0 & 0 & 0 & 0 & 0 & 0 & 0 & 0 \\ 0 & 1 & 1 & 0 & 0 & 0 & 0 & 0 & 1 & 1 & 0 & 0 & 0 & 0 & 0 & 0 & 0 & 0 & 0 & 0 \\ 0 & 1 & 1 & 0 & 0 & 0 & 0 & 0 & 0 & 1 & 1 & 0 & 0 & 0 & 0 & 0 & 0 & 0 & 0 & 0 \\ 0 & 0 & 1 & 1 & 0 & 0 & 0 & 0 & 0 & 0 & 1 & 1 & 0 & 0 & 0 & 0 & 0 & 0 & 0 & 0 \\ 0 & 0 & 1 & 1 & 0 & 0 & 0 & 0 & 0 & 0 & 0 & 1 & 1 & 0 & 0 & 0 & 0 & 0 & 0 & 0 \\ 0 & 0 & 0 & 1 & 1 & 0 & 0 & 0 & 0 & 0 & 0 & 0 & 1 & 1 & 0 & 0 & 0 & 0 & 0 & 0 \\ 0 & 0 & 0 & 1 & 1 & 0 & 0 & 0 & 0 & 0 & 0 & 0 & 0 & 1 & 1 & 0 & 0 & 0 & 0 & 0 \\ 0 & 0 & 0 & 0 & 1 & 1 & 0 & 0 & 0 & 0 & 0 & 0 & 0 & 0 & 1 & 1 & 0 & 0 & 0 & 0 \\ 0 & 0 & 0 & 0 & 1 & 1 & 0 & 0 & 0 & 0 & 0 & 0 & 0 & 0 & 0 & 1 & 1 & 0 & 0 & 0 \\ 0 & 0 & 0 & 0 & 1 & 1 & 0 & 0 & 0 & 0 & 0 & 0 & 0 & 0 & 0 & 0 & 1 & 1 & 0 & 0 \\ 0 & 0 & 0 & 0 & 1 & 1 & 0 & 0 & 0 & 0 & 0 & 0 & 0 & 0 & 0 & 0 & 0 & 1 & 1 & 0 \\ 0 & 0 & 0 & 0 & 1 & 1 & 0 & 0 & 0 & 0 & 0 & 0 & 0 & 0 & 0 & 0 & 0 & 0 & 1 & 1 \end{bmatrix}.$$

The corresponding protograph is shown in Fig. 2.

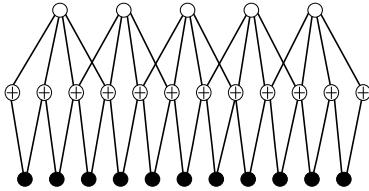


Fig. 2. Protograph corresponding to a  $(4, 2, 2, 2)$  SC-MN LDPC code ensemble. The white variable nodes are punctured.

Table I displays the BEC BP thresholds  $\varepsilon^*$  calculated for a selection of  $(4, 2, 2, L)$  SC-MN LDPCC ensembles. The AWGN channel BP thresholds obtained for both the  $(4, 2, 2, L)$  and  $(6, 3, 2, L)$  SC-MN ensembles are shown in Fig. 3.<sup>2</sup> Due to the boundary effects of coupling, there is some rate loss for finite  $L$ . The rates  $R^{MN}(4, 2, 2, L)$  and  $R^{MN}(6, 3, 2, L)$  increase monotonically and tend to  $1/k = 1/2$  as  $L \rightarrow \infty$ . The densities  $\rho^{MN}(4, 2, 2, L)$  and  $\rho^{MN}(6, 3, 2, L)$  decrease monotonically, and tend to  $J + kg = 8$  and  $J + kg = 10$  as  $L \rightarrow \infty$ , respectively, i.e., the density is bounded. We find that, for both the BEC and the AWGN channel, the iterative decoding thresholds converge to

<sup>2</sup>The (estimated) values obtained for the BP thresholds on the AWGN channel were computed using the RCA method [15].

a constant value as  $L$  gets sufficiently large and that the gap to capacity decreases with increasing  $L$ . Moreover, the obtained thresholds are close to capacity in the limit of large  $L$ .

$L$	$R^{MN}(4, 2, 2, L)$	$\rho^{MN}(4, 2, 2, L)$	$\varepsilon^*$ [13]	$\varepsilon_{Sh}$
2	0.3636	10.5	0.5611	0.6364
4	0.4211	9.25	0.5113	0.5789
8	0.4571	8.625	0.5002	0.5429
16	0.4776	8.3125	0.4999	0.5224
32	0.4885	8.1562	0.4999	0.5115

TABLE I  
BEC ITERATIVE DECODING THRESHOLDS FOR A SELECTION OF  
 $(4, 2, 2, L)$  SC-MN LDPCC ENSEMBLES.

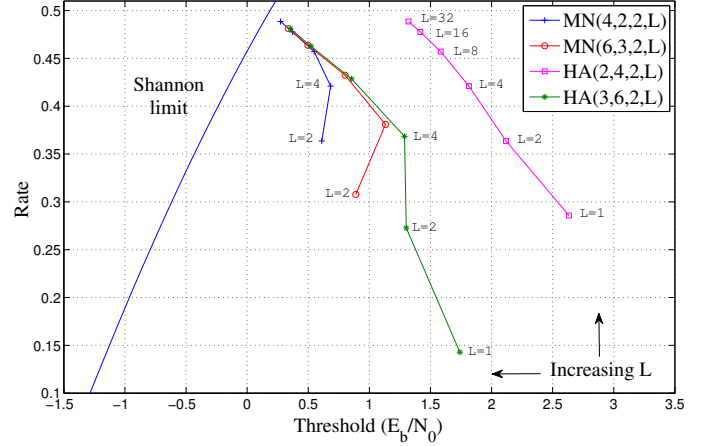


Fig. 3. AWGN channel BP thresholds for a selection of SC-MN and SC-HA LDPCC ensembles.

### B. SC-HA LDPCC ensembles

Let  $K = jJ$ ,  $J, K, g \geq 2$ , and  $L \geq 1$ , for  $J, K, g, L, j \in \mathbb{Z}$ . Suppose that we construct two SC-LDPCC base matrices  $\mathbf{F}_{[0, 2L]}$  and  $\mathbf{S}_{[0, j(2L+1)-1]}$ , in the form of (1), where the component submatrices  $\mathbf{F}_i$ ,  $i = 0, \dots, K-1$ , are each the all-ones matrix of size  $1 \times j$  and the submatrices  $\mathbf{S}_j$ ,  $j = 0, \dots, g-1$ , are each the all-ones matrix of size  $1 \times 1$  as for the MN codes. Consequently,  $\mathbf{F}_{[0, 2L]}$  has size  $(2L + J) \times j(2L + 1)$  and  $\mathbf{S}_{[0, j(2L+1)-1]}$  has size  $(j(2L + 1) + g - 1) \times j(2L + 1)$ . Then the base matrix of a  $(J, K, g, L)$  SC-HA ensemble can be written as

$$\mathbf{B}_{[0, L-1]}^{HA} = \begin{bmatrix} \mathbf{F}_{[0, 2L]} & \mathbf{0} \\ \mathbf{S}_{[0, j(2L+1)-1]} & \mathbf{I} \end{bmatrix}, \quad (5)$$

where  $\mathbf{0}$  is the all-zeros matrix of size  $(2L + J) \times (j(2L + 1) + g - 1)$ ,  $\mathbf{I}$  is the identity matrix of size  $(j(2L + 1) + g - 1) \times (j(2L + 1) + g - 1)$ , and the variable nodes associated with the left submatrix are punctured. The design rate of the ensemble is given by

$$R^{HA}(J, K, g, L) = \frac{(j-1)(2L+1) - J + 1}{j(2L+1) + g - 1}, \quad (6)$$

where

$$\lim_{L \rightarrow \infty} R^{HA}(J, K, g, L) = \frac{j-1}{j},$$

and the density of members of the ensemble is given by



$$\rho^{HA}(J, K, g, L) = \frac{j(J+g+1)(2L+1)+g-1}{j(2L+1)-2L-J}, \quad (7)$$

with

$$\lim_{L \rightarrow \infty} \rho^{HA}(J, K, g, L) = \frac{j(J+g+1)}{j-1}.$$

For example, consider the  $(2, 4, 2, 2)$  SC-HA ensemble. Here  $j = K/J = 2$ ,  $R^{HA}(2, 4, 2, 2) = 4/11$ , and  $\rho^{HA}(2, 4, 2, 2) = 51/4$ . The component submatrices are given as

$$\mathbf{F}_0 = \mathbf{F}_1 = \begin{bmatrix} 1 & 1 \end{bmatrix} \text{ and } \mathbf{S}_0 = \mathbf{S}_1 = \begin{bmatrix} 1 \end{bmatrix},$$

which are used to construct the base matrix of the  $(2, 4, 2, 2)$  SC-HA ensemble

$$\mathbf{B}_{[0, L-1]}^{HA} = \mathbf{B}_{[0, 1]}^{HA} = \begin{bmatrix} \mathbf{F}_{[0, 2L]_{6 \times 10}} & \mathbf{0}_{6 \times 11} \\ \mathbf{S}_{[0, j(2L+1)-1]_{11 \times 10}} & \mathbf{I}_{11 \times 11} \end{bmatrix}. \quad (8)$$

The corresponding protograph is shown in Fig. 4. Table II displays the BEC BP thresholds  $\varepsilon^*$  calculated for a selection of  $(2, 4, 2, L)$  SC-HA LDPCC ensembles. The rate  $R^{HA}(2, 4, 2, L)$  increases monotonically and tends to  $(j-1)/j = 1/2$  as  $L \rightarrow \infty$ . The density  $\rho^{HA}(2, 4, 2, L)$  decreases monotonically and tends to  $j(J+g+1)/(j-1) = 10$  as  $L \rightarrow \infty$ , i.e., the density is bounded. Note that  $R^{HA}(2, 4, 2, L) = R^{MN}(4, 2, 2, L) = 2L/(4L+3)$ ; however, we see that the density of the SC-HA ensemble is larger. From Fig. 3, we observe that the thresholds obtained for the  $(2, 4, 2, L)$  SC-HA LDPCC ensembles on the AWGN channel show a significant gap to capacity. However, the thresholds of the  $(3, 6, 2, L)$  SC-HA LDPCC ensembles display similar characteristics to the SC-MN ensembles and converge to a constant value close to capacity in the limit of large  $L$ .

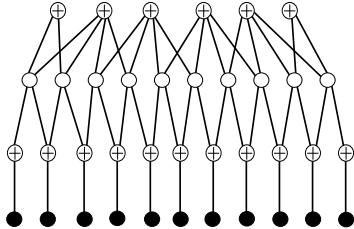


Fig. 4. Protograph corresponding to a  $(2, 4, 2, 2)$  SC-HA LDPC code ensemble. The white variable nodes are punctured.

$L$	$R^{HA}(2, 4, 2, L)$	$\rho^{HA}(2, 4, 2, L)$	$\varepsilon^*$ [13]	$\varepsilon_{Sh}$
1	0.2857	15.5	0.6954	0.7143
2	0.3636	12.75	0.5944	0.6364
4	0.4211	11.375	0.5169	0.5789
8	0.4571	10.6875	0.5004	0.5429
16	0.4776	10.3438	0.4999	0.5224
32	0.4885	10.1719	0.4999	0.5115

TABLE II  
BEC ITERATIVE DECODING THRESHOLDS FOR A SELECTION OF  
 $(2, 4, 2, L)$  SC-HA LDPCC ENSEMBLES.

#### IV. MINIMUM DISTANCE ANALYSIS OF SC-MN AND SC-HA LDPCC ENSEMBLES

In this section, we study the minimum distance of SC-MN and SC-HA LDPCC ensembles. The *asymptotic spectral*

*shape function* of a code ensemble is given by  $r(\delta) = \lim_{n \rightarrow \infty} \sup r_n(\delta)$ , where  $r_n(\delta) = \ln(A_d)/n$ ,  $\delta = d/n$ ,  $d$  is the Hamming weight,  $n$  is the block length, and  $A_d$  is the ensemble average weight distribution. Suppose that the first positive zero crossing of  $r(\delta)$  occurs at  $\delta = \delta_{min}$ . If  $r(\delta)$  is negative in the range  $0 < \delta < \delta_{min}$ , then  $\delta_{min}$  is called the *minimum distance growth rate* of the code ensemble. By considering the probability  $\mathbb{P}(d < n\delta_{min}) \leq \sum_{d=1}^{n\delta_{min}-1} A_d$ , it is clear that, as the block length  $n$  becomes sufficiently large, if  $\mathbb{P}(d < n\delta_{min}) \ll 1$ , then we can say with high probability that a randomly chosen code from the ensemble has a minimum distance that is at least as large as  $n\delta_{min}$  [16], i.e., the minimum distance increases linearly with block length  $n$ . We refer to such an ensemble of codes as *asymptotically good*. The asymptotic spectral shape function  $r(\delta)$  of a protograph-based LDPC code ensemble can be calculated using the techniques presented by Divsalar et al. in [16].

##### A. Asymptotic distance analysis of SC-MN LDPCC ensembles

Consider the  $(4, 2, 2, 2)$  SC-MN LDPC code ensemble previously discussed in Section III-A. The asymptotic spectral shape function for this ensemble is plotted in Fig. 5. We see that this ensemble is asymptotically good and that the minimum distance growth rate is  $\delta_{min} = 0.022$ .

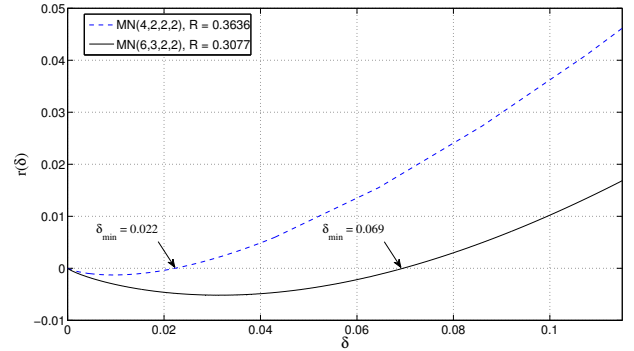


Fig. 5. Asymptotic spectral shape functions for the  $(4, 2, 2, 2)$  and  $(6, 3, 2, 2)$  SC-MN LDPC code ensembles.

As we increase the coupling length  $L$ , the rate increases, and the calculated BP thresholds get closer to capacity (see Table I and Fig. 3). The minimum distance growth rates, on the other hand, decrease with  $L$ , as shown in Fig. 6 for  $L = 2, 3, \dots, 8$ . Numerically, it becomes problematic to evaluate  $\delta_{min}$  for large values of  $L$ ; however, it is clear from the structure of the ensembles that the growth rates continue to decrease and tend to zero in the limit of large  $L$  if the coupling width is fixed.

Now consider increasing the density of the punctured variable nodes. The asymptotic spectral shape function for the  $(6, 3, 2, 2)$  SC-MN code ensemble is plotted in Fig. 5. We see that this ensemble is asymptotically good and that the minimum distance growth rate is significantly larger than for the  $(4, 2, 2, 2)$  SC-MN code ensemble. Fig. 6 shows the minimum distance growth rates obtained for the  $(6, 3, 2, L)$  SC-MN ensembles for  $L = 2, 3, \dots, 8$ . We observe a significant increase in the growth rates by increasing  $J$  and  $K$  while maintaining thresholds close to capacity (see Fig. 3). Analogously to  $(J, K)$ -regular LDPC block code ensembles,

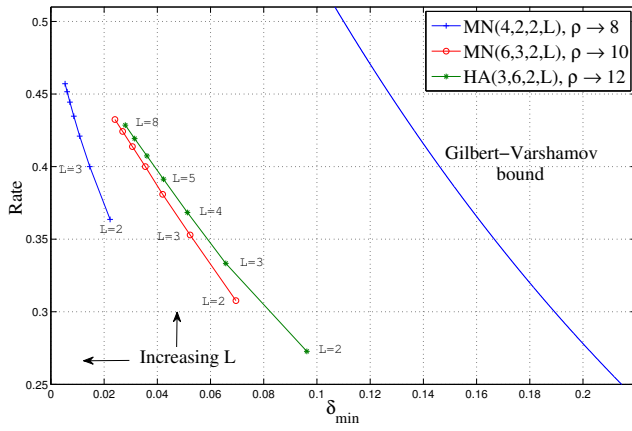


Fig. 6. Minimum distance growth rates for a selection of SC-MN and SC-HA LDPC ensembles. The parameter  $\rho$  indicates the ensemble density obtained in the limit of large  $L$ .

we expect to observe increased minimum distance growth rates as we continue to increase  $J$  and  $K$ .

### B. Asymptotic distance analysis of SC-HA LDPC ensembles

Consider the  $(2, 4, 2, 2)$  SC-HA LDPC code ensemble previously discussed in Section III-B. The asymptotic spectral shape function for this ensemble is plotted in Fig. 7 along with the results for coupling lengths  $L = 1$  and  $L = 4$ . The asymptotic spectral shape functions for these ensembles indicate that they are not asymptotically good. (Recall also that the AWGN channel thresholds displayed a significant gap to capacity for these ensembles (see Fig. 3).)

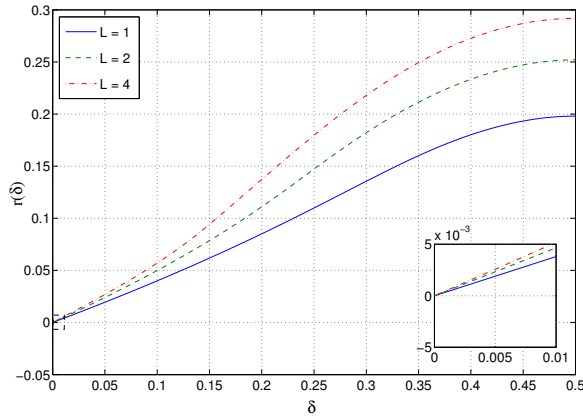


Fig. 7. Asymptotic spectral shape functions for  $(2, 4, 2, L)$  SC-HA LDPC code ensembles with  $L = 1, 2$ , and  $4$ .

Fig. 6 displays the calculated growth rates for several  $(3, 6, 2, L)$  SC-HA LDPC ensembles. We observe that, by increasing the density of the punctured variable nodes, in addition to obtaining BP thresholds close to capacity for both the BEC and the AWGN channel, the SC-HA LDPC ensembles are asymptotically good. Comparing the  $(6, 3, 2, L)$  SC-MN ensembles and  $(3, 6, 2, L)$  SC-HA ensembles, we find that the rates of both families of SC-LDPC ensembles approach  $1/2$  with BP thresholds close to capacity; however,

the minimum distance growth rates of the SC-HA codes are larger, which can be attributed in part to their higher density.

## V. CONCLUSIONS

In this paper, we have performed an asymptotic analysis of spatially coupled MacKay-Neal and Hsu-Anastasopoulos LDPC codes. We demonstrated that, for both the BEC and the AWGN channel, the BP thresholds of the SC-MN and SC-HA ensembles are close to capacity with bounded density as the coupling length increases, i.e., the number of edges per information bit approaches a finite value as the estimated BP threshold approaches the Shannon limit. By performing an asymptotic weight enumerator analysis, we also showed that, provided that the density parameters are chosen to be sufficiently large, the SC-MN and SC-HA ensembles are asymptotically good. Further, for certain selections of parameters, some of these ensembles are shown to have both excellent thresholds and large minimum distance growth rates.

## REFERENCES

- [1] M. Lentmaier, G. P. Fettweis, K. Sh. Zigangirov, and D. J. Costello, Jr., "Approaching capacity with asymptotically regular LDPC codes," in *Proc. Inf. Theory and App. Workshop*, San Diego, CA, Feb. 2009.
- [2] M. Lentmaier, A. Sridharan, D. J. Costello, Jr., and K. Sh. Zigangirov, "Iterative decoding threshold analysis for LDPC convolutional codes," *IEEE Trans. Inf. Theory*, vol. 56, no. 10, pp. 5274–5289, Oct. 2010.
- [3] M. Lentmaier, D. G. M. Mitchell, G. P. Fettweis, and D. J. Costello, Jr., "Asymptotically good LDPC convolutional codes with AWGN channel thresholds close to the Shannon limit," in *Proc. 6th Int. Symp. on Turbo Codes and Iterative Inf. Processing*, Brest, France, Sept. 2010.
- [4] S. Kudekar, C. Méasson, T. Richardson, and R. Urbanke, "Threshold saturation on BMS channels via spatial coupling," in *Proc. 6th Int. Symp. Turbo Codes and Iterative Inf. Processing*, Brest, France, Sept. 2010.
- [5] S. Kudekar, T. J. Richardson, and R. L. Urbanke, "Threshold saturation via spatial coupling: why convolutional LDPC ensembles perform so well over the BEC," *IEEE Trans. Inf. Theory*, vol. 57, no. 2, pp. 803–834, Feb. 2011.
- [6] S. Kudekar, T. J. Richardson, and R. L. Urbanke, "Spatially Coupled Ensembles Universally Achieve Capacity Under Belief Propagation," [Online.] <http://arxiv.org/abs/1201.2999>, 2012.
- [7] G. Miller and D. Burshtein, "Bounds on the maximum-likelihood decoding error probability of low-density parity-check codes," *IEEE Trans. Inf. Theory*, vol. 47, no. 7, pp. 2696–2710, Nov. 2001.
- [8] D. J. C. MacKay and R. M. Neal, *Good codes based on very sparse matrices*, ser. in "Lecture Notes in Computer Science". Berlin: Springer, 1995, no. 1025, pp. 100–111.
- [9] D. J. C. MacKay, "Good error-correcting codes based on very sparse matrices," *IEEE Trans. Inf. Theory*, vol. 45, no. 2, pp. 399–431, Mar. 1999.
- [10] C. Hsu and A. Anastasopoulos, "Capacity-achieving codes with bounded graphical complexity and maximum likelihood decoding," *IEEE Trans. Inf. Theory*, vol. 56, no. 3, pp. 992–1006, Mar. 2010.
- [11] T. Murayama, Y. Kabashima, D. Saad, and R. Vicente, "Statistical physics of regular low-density parity-check error-correcting codes," *Phys. Rev. E*, vol. 62, no. 2, pp. 1577–1591, Aug. 2000.
- [12] T. Tanaka and D. Saad, "Typical performance of regular low-density parity-check codes over general symmetric channels," *J. Phys. A: Math. and Gen.*, vol. 36, no. 43, pp. 11 143–11 157, Oct. 2003.
- [13] K. Kasai and K. Sakaniwa, "Spatially-coupled MacKay-Neal codes and Hsu-Anastasopoulos codes," in *Proc. IEEE Int. Symp. on Inf. Theory*, St. Petersburg, Russia, Aug. 2011.
- [14] J. Thorpe, "Low-density parity-check (LDPC) codes constructed from protographs," Jet Propulsion Laboratory, Pasadena, CA, INP Progress Report 42-154, Aug. 2003.
- [15] S.-Y. Chung, "On the construction of some capacity-approaching coding schemes," Ph.D. dissertation, Massachusetts Institute of Technology, Cambridge, MA, Sept. 2000.
- [16] D. Divsalar, S. Dolinar, C. Jones, and K. Andrews, "Capacity-approaching protograph codes," *IEEE Jour. Sel. Areas in Comm.*, vol. 27, no. 6, pp. 876–888, Aug. 2009.